MULTIBODY DYNAMICS 2009, ECCOMAS Thematic Conference
K. Arczewski, J. Frączek, M. Wojtyra (eds.)
Warsaw, Poland, 29 June–2 July 2009

DISCRETE LAGRANGIAN MECHANICS AND GEOMETRICALLY EXACT COSSERAT RODS

Pascal Jung[⋆], Sigrid Leyendecker[†], Joachim Linn[‡] and Michael Ortiz[§]

[⋆]University of Kaiserslautern
Erwin Schrödinger Straße, 67663 Kaiserslautern, Germany
e-mail: pjung@mathematik.uni-kl.de

[†]Freie Universität Berlin
Arnimalle 6, 14195 Berlin, Germany
e-mail: sleye@zedat.fu-berlin.de

[‡]Fraunhofer ITWM
Fraunhofer Platz 1, 67663 Kaiserslautern, Germany
e-mail: linn@itwm.fraunhofer.de

[§]California Institute of Technology
1200 E California Blvd, 91125 Pasadena, CA, USA
e-mail: ortiz@aero.caltech.edu

Keywords: Special Cosserat rods, Lagrangian mechanics, Noether's theorem, discrete mechanics, frame-indifference, holonomic constraints.

Abstract. *Inspired by Kirchhoff's kinetic analogy, the special Cosserat theory of rods is formulated in the language of Lagrangian mechanics. A static rod corresponds to an abstract Lagrangian system where the energy density takes the role of the Lagrangian function. The equilibrium equations are derived from a variational principle. Noether's theorem relates their first integrals to frame-indifference, isotropy and uniformity. These properties can be formulated in terms of Lie group symmetries. The rotational degrees of freedom, present in the geometrically exact beam theory, are represented in terms of orthonormal director triads. To reduce the number of unknowns, Lagrange multipliers associated with the orthonormality constraints are eliminated using null-space matrices. This is done both in the continuous and in the discrete setting. The discrete equilibrium equations are used to compute discrete rod configurations, where different types of boundary conditions can be handled.*

1 INTRODUCTION

In the past two decades, the theory of discrete mechanics (see Ref. [1]) has grown to be a large and interesting area of research. Numerical integrators that are derived from a discrete variational principle have favourable conservation properties. The fact that the equations of motion for a Lagrange top are formally equivalent to the equilibrium equations of an isotropic Kirchhoff rod is known in the literature as Kirchhoff's kinetic analogy and attempts have been taken to generalize Kirchhoff's kinetic analogy to Cosserat rod models. Examples of such investigations can be found in Ref. [2] and Ref. [3] where a variety of Hamiltonian systems are constructed whose canonical equations correspond to the equilibrium equations of the respective rod model.

It is an interesting idea to apply the theory of geometric integrators to mechanical systems that arise in the context of such kinetic analogies and analyze the properties of the discretizations obtained that way. Such approaches have been taken for example in Ref. [4] or in Ref. [5]. The aim of this article is the systematic application of concepts from classical and discrete mechanics in order to describe hyperelastic rods both in the continuous and in the discrete setting.

The potential energy density is the object of most importance in rod theory. In the case of hyperelastic material behavior, it specifies the constitutive properties of the rod and implies the constitutive equations which relate strains to forces and moments. Kirchhoff's kinetic analogy suggests that this energy density function (depending on the space curve parameter) is formally equivalent to the Lagrangian function of a time-dependent mechanical system, such that the static equilibrium equations of a rod correspond to the Euler-Lagrange equations of the latter.

When deriving the equilibrium equations by computing variations of the potential energy, two aspects deserve special attention. First of all, the canonical expressions for the strain vectors imply that the internal energy (which is associated to strain) is invariant under rigid motions. This invariance property is called objectivity or frame-indifference. It is shown in Ref. [6] that frame-indifference is the basic requirement for the spatial Euler-Lagrange equations to take the familiar form of Eq. (9). Frame-indifference also ensures the existence of six first integrals that can be recovered as momentum maps in the context of Noether's theorem. It is crucial that frame-indifference is preserved in a discrete rod model because the aforementioned features have equivalents in the discrete setting. Secondly, since due to the presence of rotations the configuration manifold corresponding to a Cosserat rod is not a vector space, we have to deal with Lagrange multipliers in the equilibrium equations. In the present work, we use an equivalent formulation involving null-space matrices based on the ideas in Ref. [7].

The discrete mechanics part is developed fairly analogously. Based on a discretization of the variational principle, the discrete equilibrium equations are derived which exhibit a similar stucture as the continuous equations (assumed that the discretization is frame-indifferent!). This set of equations will be the basis for numerical algorithms.

2 VARIATIONAL FORMULATION OF ROD THEORY

2.1 Basic kinematics

A configuration of a continuous Cosserat rod is determined by a vector function $r : [0, L] \rightarrow \mathbb{R}^3$, together with a pair $d^{(1)}, d^{(2)} : [0, L] \rightarrow \mathbb{R}^3$ of vector functions that satisfy the orthonormality conditions $\langle d^{(1)}(s), d^{(2)}(s) \rangle = 0$, $\|d^{(k)}(s)\|_2 = 1$ for $k = 1, 2$, $s \in [0, L]$. While r addresses points on the centerline, the $d^{(k)}$ describe the orientation of the cross-section along $[0, L]$. We define the cross-section normal vector $d^{(3)}(s) = d^{(1)}(s) \times d^{(2)}(s)$ to obtain a right-handed orthonormal basis $(d^{(1)}, d^{(2)}, d^{(2)})$, called director field. The deformed configuration can

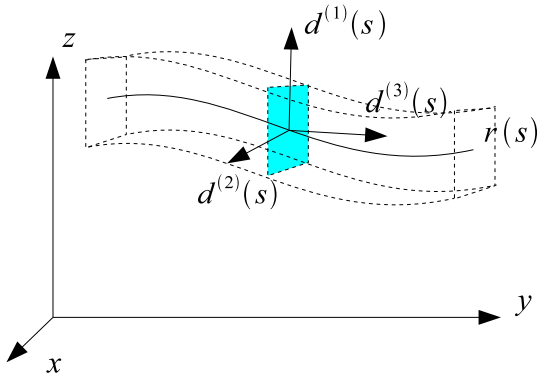

Figure 1: Kinematics of a special Cosserat rod in terms of centerline and directors.

alternatively be described by the pair (r, R)

$$(r, R) : [0, L] \to \mathbb{R}^3 \times \mathrm{SO}(3)$$

where $R(s) = [d^{(1)}(s), d^{(2)}(s), d^{(3)}(s)] \in \mathrm{SO}(3)$ denotes the column matrix corresponding to the director field. The full kinematical information is therefore given by a curve in the manifold $Q = \mathbb{R}^3 \times \mathrm{SO}(3)$.

2.2 Submanifolds and null-space matrices

As mentioned in the introduction, due to the presence of rotations, Q is not a vector-space. However, we work with the embedding of Q in $\mathbb{R}^{12}$ giving rise to constraints. Our formulation of rod theory involves null-space matrices, which we prefer to the formulation with Lagrange multipliers. A null-space matrix at $q \in Q$ is a matrix $P(q) \in \mathbb{R}^{12\times 6}$ such that $\mathrm{range}(P(q)) = T_qQ$. An important feature of null-space matrices is that they can be used to eliminate constraint "forces" that arise due to the constraints induced by Q. See Ref. [7, 8, 9] for further details. We choose

$$P(q) = \begin{bmatrix} \mathbb{1}_3 & 0 \\ 0 & -\hat{d}^{(1)} \\ 0 & -\hat{d}^{(2)} \\ 0 & -\hat{d}^{(3)} \end{bmatrix} \quad \text{for} \quad q = \begin{bmatrix} r \\ d^{(1)} \\ d^{(2)} \\ d^{(3)} \end{bmatrix} \in Q \tag{1}$$

where we denote by $\hat{d} \in \mathrm{so}(3)$ the skew-symmetric matrix corresponding to $d \in \mathbb{R}^3$ defined through the relation $\hat{d}\, y = d \times y$ for all $y \in \mathbb{R}^3$.

2.3 Potential energy and frame-indifference

Frame-indifferent strain measures can be defined as follows:

$$\hat{\mathbf{u}} = R^{-1}\frac{\mathrm{d}}{\mathrm{d}s}R, \qquad \mathbf{v} = R^{-1}\frac{\mathrm{d}}{\mathrm{d}s}r \tag{2}$$

Precisely, frame-indifference means invariance under the transformations

$$r \mapsto y + r, \qquad y \in \mathbb{R}^3, \tag{3}$$

$$(r, R) \mapsto (Yr, YR), \qquad Y \in \mathrm{SO}(3) \tag{4}$$

Thus we obtain six components of strain: the (non-zero) entries of $\hat{\mathbf{u}}$ and $\mathbf{v}$ describe flexure, twist, shear and stretch. Associated with the strains, we have a stress force $n(s)$ and a stress moment $m(s)$ at $r(s)$.

We assume that we deal with a hyperelastic material. In view of (2), we define a function

$$W : TQ \to \mathbb{R} \tag{5}$$

which models the potential energy density (energy per unit of reference length). The energy density $W = W^{\text{int}} + W^{\text{ext}}$ splits into an internal component W^{int}, associated to the strain vectors $\mathbf{u}$ and $\mathbf{v}$ and an external component W^{ext} associated to external loads such as gravity. It is required that W^{int} is frame-indifferent.

2.4 Equilibrium equations

For hyperelastic materials, the (spatial) forces and moments are given by the constitutive equations

$$n = \frac{\partial W^{\text{int}}}{\partial r'}, \qquad m = \sum_{k=1}^{3} d^{(k)} \times \frac{\partial W^{\text{int}}}{\partial d^{(k)\prime}}\,. \tag{6}$$

It can be shown that Eq. (6) is an equivalent formulation of the hyperelastic constitutive equations Eq. (4.12) in Ref. [10]. The equilibrium configurations of any static system coincide with the critical points of the potential energy. This means, for hyperelastic rods, a (stable or unstable) equilibrium configuration satisfies

$$\delta \int_0^L W\left(q(s), \frac{\mathrm{d}}{\mathrm{d}s} q(s)\right) \mathrm{d}s = 0\,. \tag{7}$$

Eq. (7) formally corresponds to Hamilton's principle of critical action, yet the physical dimension of the integral is energy and integration is taken with respect to the curve parameter s. The corresponding spatial Euler-Lagrange equations, derived by variational calculus, read

$$P(q)^T \left(\frac{\mathrm{d}}{\mathrm{d}s}\frac{\partial W}{\partial q'} - \frac{\partial W}{\partial q}\right) = 0 \tag{8}$$

with $q \in Q$ and $P(q)$ as chosen in Sect. 2.2. The details of the derivation are omitted and can be found in Ref. [6] and in Ref. [9]. Exploiting the assumption of frame-indifference and using the expressions in Eq. (6), one can also show that Eq. (8) can be written in the classical form

$$\frac{\mathrm{d}}{\mathrm{d}s} n + f = 0 \tag{9a}$$

$$\frac{\mathrm{d}}{\mathrm{d}s} m + \frac{\mathrm{d}}{\mathrm{d}s} r \times n + l = 0 \tag{9b}$$

where f and l denote the external forces and moments, respectively. Different derivations of these equations can be found in the literature. In Ref. [11] it is shown that they follow from Newton's Law, and in Ref. [10] they are derived from the three-dimensional continuum theory.

2.5 Spatial symmetries and momentum maps

Consider the action of a Lie group G on Q, denoted by $\Phi : G \times Q \to Q$. Further, let $\mathfrak{g}$ denote the Lie algebra corresponding to G. Φ is called a symmetry if W is invariant under

transformations by Φ. In particular, this implies that for any $\xi \in \mathfrak{g}$, the pointwise transformation of a configuration map q by $\exp(\varepsilon\xi)$ generates a family $(q_\varepsilon)_{\varepsilon\in\mathbb{R}}$

$$q_\varepsilon(s) = \Phi(\exp(\varepsilon\xi), q(s)), \qquad s \in [0, L]$$

where all q_ε have the same potential energy. Eq. (3) and Eq. (4) already give two examples of symmetries for Cosserat rods. By Noether's theorem, any symmetry results in a spatially (along the center line of the rod) conserved quantity, called first integral or momentum map. Given an energy density W and a group action Φ, the corresponding momentum map is given by

$$J(q, q')\,\xi = \left\langle \frac{\partial W}{\partial q'}, \xi_Q(q) \right\rangle, \qquad \xi \in \mathfrak{g}$$

where

$$\xi_Q(q) = \frac{\mathrm{d}}{\mathrm{d}\varepsilon}\Phi(\exp(\varepsilon\xi), q)\bigg|_{\varepsilon=0} \qquad \in T_qQ$$

denotes the infinitesimal generator. It is known, that a Cosserat rod has up to 8 scalar first integrals, depending on its constitutive properties. In the case of frame-indifference (that is, if $f = l = 0$), the stress force n and the momentum quantity $m + r \times n$ are conserved. Moreover if W is invariant under rotations of the director field about $d^{(3)}$ - this feature is termed isotropy - then the twist moment $\langle m, d^{(3)}\rangle$ is conserved.

Remark 2.1 *The rods that can be described by the above theory are uniform because in Eq.* (5) W *"does not depend explicitly on* s*". As a consequence, the quantity* $\langle n, r'\rangle + \langle m, u\rangle - W$ *is conserved. In order to describe non-uniform rods and properly define uniformity, we need to extend the domain of* W *to* $\mathbb{R} \times TQ$*. In this introductory paper we restrict ourselves to the uniform theory and refer the interested reader to Ref. [1] and Ref. [6].*

3 DISCRETE ROD THEORY

3.1 Discrete kinematics

A discrete configuration (of a rod) is given by a sequence

$$(q_1 \dots q_N), \qquad q_i = (r_i, d_i^{(1)}, d_i^{(2)}, d_i^{(3)}) \in Q$$

which is associated with an equidistant grid $\{s_i = (i-1)\cdot h \,|\, i = 1 \dots N\}$, $h = L/(N-1)$ for a beam of length L with N nodes.

3.2 Potential energy sum and equilibrium equations

The discrete object corresponding to TQ is the product $Q \times Q$ and the potential energies of the $N-1$ segments are modeled by a sequence

$$W_i : Q \times Q \to \mathbb{R}$$

Remark 3.1 *When constructing numerical methods from discrete mechanics, it is crucial to find a "good" choice for* W_i *such that the discrete energy sum is a reasonable approximation of the continous energy integral and inherits additional features, e.g. invariance properties. In particular, for rods, a discretization of the energy integral involves discrete strain vectors* $\mathbf{u}_i, \mathbf{v}_i : Q \times Q \to \mathbb{R}^3$ *whose choice is non-canonical.*

Analogously to the continuous case, it is assumed that each $W_i = W_i^{\text{int}} + W_i^{\text{ext}}$ splits into a frame-indifferent component W_i^{int}, the strain energy, and a component W_i^{ext}, the energy induced by external loads.

Discrete forces and moments are defined as follows:

$$n_i = -\frac{\partial W_i^{\text{int}}}{\partial r_i} \left(= \frac{\partial W_i^{\text{int}}}{\partial r_{i+1}} \right), \quad m_i^- = -\sum_{k=1}^{3} d_i^{(k)} \times \frac{\partial W_i^{\text{int}}}{\partial d_i^{(k)}}, \quad m_i^+ = \sum_{k=1}^{3} d_{i+1}^{(k)} \times \frac{\partial W_i^{\text{int}}}{\partial d_{i+1}^{(k)}} \tag{10}$$

Here, m_i^+ and m_i^- can be thought of as two different discretizations of the stress moment. The fact that W_i^{int} is frame-indifferent implies that there is only one discrete force. Equilibrium configurations are characterized by the variational principle

$$\delta \sum_{i=1}^{N-1} W_i(q_i, q_{i+1}) = 0 \tag{11}$$

which is equivalent to the set

$$P(q_i)^T \left(\frac{\partial W_{i-1}}{\partial q_i} + \frac{\partial W_i}{\partial q_i} \right) = 0 \tag{12}$$

of discrete Euler-Lagrange equations (possibly extended by additional equations corresponding to certain boundary data). It is shown in Ref. [6] that Eq. (12) can alternatively be written as

$$n_i - n_{i-1} + f_i = 0 \tag{13a}$$

$$m_i^- - m_{i-1}^- + (r_i - r_{i-1}) \times n_{i-1} + l_i = 0 \tag{13b}$$

$$m_i^+ - m_{i-1}^+ + (r_{i+1} - r_i) \times n_i + l_i = 0 \tag{13c}$$

where (13b) and (13c) are equivalent. In parallel to the previous section, there exists a discrete version of Noether's theorem.

3.3 Spatial symmetries and momentum maps

Consider a Lie group action $\Phi : G \times Q \to Q$ which leaves W_i invariant. For any $\xi \in \mathfrak{g}$, we can construct a family

$$q_{i,\varepsilon} = \Phi(\exp(\varepsilon\xi), q_i)$$

of configuration variables with $W_i(q_i, q_{i+1}) = W_i(q_{\varepsilon,i}, q_{\varepsilon,i+1})$. The discrete Noether's theorem (see Ref. [1]) states that in this case, there exists a sequence of momentum maps

$$J_i(q_i, q_{i+1})\xi = -\left\langle \frac{\partial W_i}{\partial q_i}, \xi_Q(q_i) \right\rangle = \left\langle \frac{\partial W_i}{\partial q_{i+1}}, \xi_Q(q_{i+1}) \right\rangle, \qquad \xi \in \mathfrak{g}$$

which is conserved along $q_1 \dots q_N$. The J_i can be interpreted as natural discretizations of the four expressions for the continuous momentum maps. By inserting the respective expressions

for ξ_Q we compute

$$J_i = n_i \qquad \text{(frame-indifference)} \qquad (14)$$

$$J_i = m_i^- + r_i \times n_i = m_i^+ + r_{i+1} \times n_i \qquad \text{(frame-indifference)} \qquad (15)$$

$$J_i = \left\langle \frac{\partial W_i}{\partial d_{i+1}^{(1)}}, d_{i+1}^{(2)} \right\rangle - \left\langle \frac{\partial W_i}{\partial d_{i+1}^{(2)}}, d_{i+1}^{(1)} \right\rangle \qquad (16)$$

$$= \left\langle \frac{\partial W_i}{\partial d_i^{(2)}}, d_i^{(1)} \right\rangle - \left\langle \frac{\partial W_i}{\partial d_i^{(1)}}, d_i^{(2)} \right\rangle \qquad \text{(isotropy)} \qquad (17)$$

$$J_i = \frac{\partial W_i}{\partial s_{i+1}} = -\frac{\partial W_i}{\partial s_i} \qquad \text{(uniformity)} \qquad (18)$$

Remark 3.2 *For the correct formulation of uniformity it is convenient to allow non-equidistant grids and to define the energy functions on* $\mathbb{R} \times Q \times \mathbb{R} \times Q$. *For the full treatment we refer again to Ref. [1] and Ref. [6].*

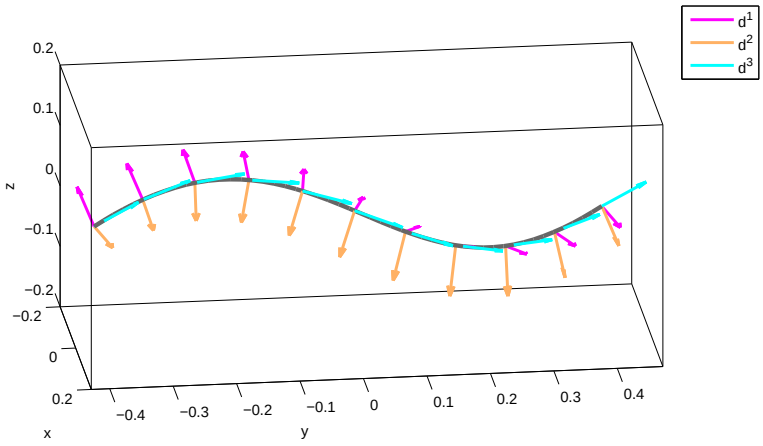

Figure 2: Deformed configuration with 11 vertices.

4 DISCRETIZATION AND NUMERICAL RESULTS

4.1 Three-dimensional equilibria

In this section, possible discretizations and their implementations are discussed which fill the discrete mechanics framework from Sect. 3 so that discrete configurations can actually be computed. First, we choose an appropriate quadrature rule for the energy functional where we restrict ourselves to discretizations of the following energy functional:

$$V = \frac{1}{2}\int_0^L \langle \mathbf{u} - \mathbf{u}^0, C_1(\mathbf{u} - \mathbf{u}^0)\rangle \, \mathrm{d}s + \frac{1}{2}\int_0^L \langle \mathbf{v} - \mathbf{v}^0, C_2(\mathbf{v} - \mathbf{v}^0)\rangle \, \mathrm{d}s \qquad (19)$$

Here, $\mathbf{u}^0, \mathbf{v}^0 \in \mathbb{R}^3$ describe the predeformed configuration and $C_1, C_2 \in \mathbb{R}^{3\times 3}$ are symmetric and positive definite matrices, called stiffness matrices. Essentially, this reduces to the task of

finding discrete strain vectors $\mathbf{u}_i, \mathbf{v}_i$. Here, we present a possible choice in an ad-hoc manner:

$$\mathbf{u}_i = \frac{2}{h}\frac{1}{1+\mathrm{trace}(R_i^{-1}R_{i+1})}(R_i^{-1}R_{i+1} - R_{i+1}^{-1}R_i) \tag{20}$$

$$\mathbf{v}_i = \frac{1}{2h}(R_{i+1}^{-1} + R_i^{-1})(r_{i+1} - r_i) \tag{21}$$

Note that Eq. (20) and Eq. (21) are consistent discretizations of the continuum strain measures in Eq. (2) located at $\frac{1}{2}(s_i + s_{i+1})$. Now, Eq. (19) can be approximated using the midpoint rule:

$$V^d = \frac{1}{2}\sum_{i=1}^{N-1}\langle \mathbf{u}_i - \mathbf{u}_i^0, C_1(\mathbf{u}_i - \mathbf{u}_i^0)\rangle h + \frac{1}{2}\sum_{i=1}^{N-1}\langle \mathbf{v}_i - \mathbf{v}_i^0, C_2(\mathbf{v}_i - \mathbf{v}_i^0)\rangle h \tag{22}$$

Thus, we obtain a frame-indifferent and consistent discretization of the energy functional.

Remark 4.1 *This discretization is very much the same as a finite element method using linear finite elements and numerical integration via the midpoint rule, see e.g. [12]. However, the factor involving the trace in Eq.* (20) *is different. Its singularity at the relative rotation between neighboring director triads of* π *enables the method to cope with relatively large applied momentum loads.*

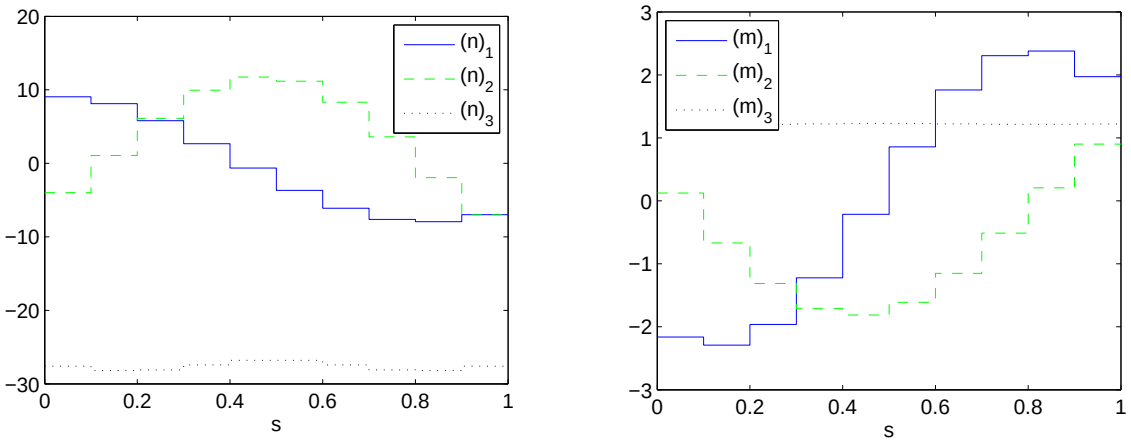

(a) (b)

Figure 3: (a) The discrete forces $\mathbf{n}_i$. (b) The discrete moments $\mathbf{m}_i$.

In the following, we treat a boundary value problem, where both ends of a straight rod are clamped. The main focus is on the spatial momentum maps and on convergence properties. We choose boundary data that result in a non-trivial deformation which exhibits non-zero twist, extension, flexure and shear:

$$r_0 = \begin{pmatrix} 0 \\ -0.4 \\ 0 \end{pmatrix}, \quad r_L = \begin{pmatrix} 0 \\ 0.4 \\ 0 \end{pmatrix}, \quad d_0^{(3)} = d_L^{(3)} = \begin{pmatrix} -0.18070 \\ 0.89768 \\ 0.40187 \end{pmatrix}$$

$$d_0^{(1)} = -d_L^{(2)} = \begin{pmatrix} 0.21093 \\ -0.36372 \\ 0.90731 \end{pmatrix}, \quad d_0^{(2)} = d_L^{(1)} = \begin{pmatrix} 0.96065 \\ 0.24872 \\ -0.12363 \end{pmatrix}$$

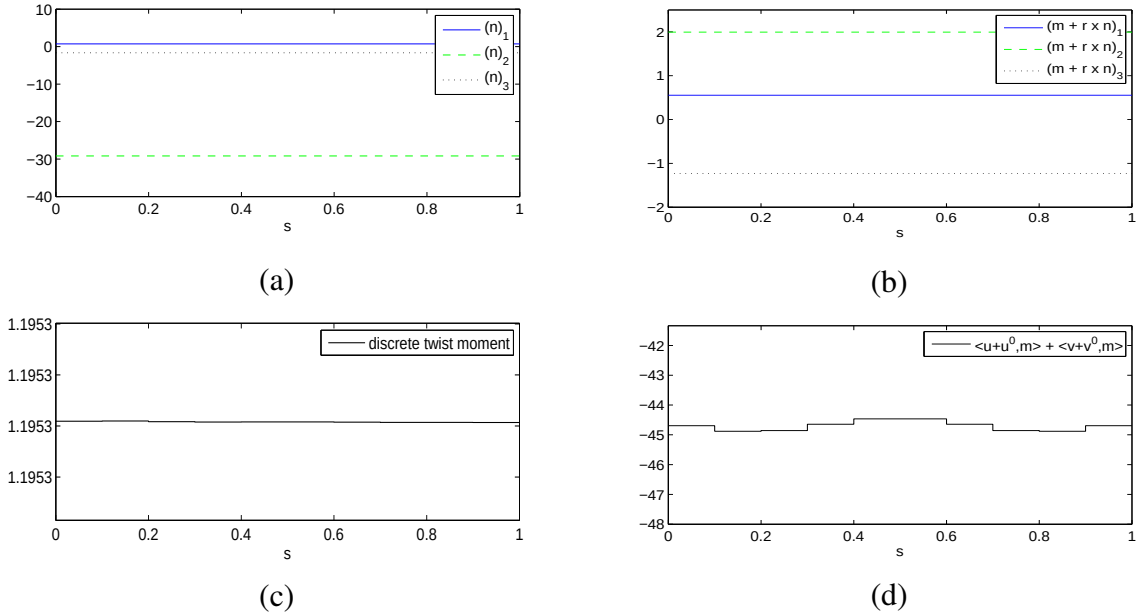

Figure 4: The discrete momentum maps associated to (a),(b) frame-indifference, (c) isotropy and (d) uniformity on an equidistant grid.

Practically any boundary data would work here because the actual shape of the deformation has no influence on the fact that momentum maps are conserved.

We implement the model given by Eq. (20), (21) and (22) involving diagonal stiffness matrices $C_1 = \mathrm{diag}(EI, EI, GJ)$, $C_2 = \mathrm{diag}(GA, GA, EA)$ and $\mathbf{u}^0 = (0,0,0)^T$, $\mathbf{v}^0 = (0,0,1)^T$, corresponding to an initially straight rod. The stiffness parameters are $EI = 1$, $GJ = 1$, $GA = 200$ and $EA = 200$. The rod of length $L = 1$ is equidistantly discretized into $N = 11$ material points, thus $h = 0.1$.

We compute the deformed configuration by solving the system in Eq. (12) subject to the constraints $\langle d_i^{(k)}, d_i^{(j)} \rangle = \delta_{kj}$ using a Gauss-Newton iteration (Matlab-function `fsolve`) and a finite-difference approximation of the Jacobi-matrix. The tolerance of the algorithm is set to 10^{-8}. The initial guess is simply a spline generated from the boundary data.

Fig. 2 depicts the deformed configuration with the director frame at each node. The discrete forces $\mathbf{n}_i = C_2(\mathbf{v}_i - \mathbf{v}_i^0)$ and moments $\mathbf{m}_i = C_1(\mathbf{u}_i - \mathbf{u}_i^0)$ are discrete pendants of *material* quantities (see Section 3.1 in Ref. [10]) and are therefore different from the *spatial* forces and moments in Eq. (10). Fig. 3 displays the six components of $\mathbf{n}_i$ and $\mathbf{m}_i$. Since the stiffness matrices are diagonal, each component is associated to a specific component of strain. For example $(\mathbf{m}_i)_3$ is the twist moment. Note that in the discrete setting, $(\mathbf{m}_i)_3$ is not a momentum map, although as we can see from Fig. 3 (b) that it is "almost" conserved. Fig. 4 shows the four momentum maps mentioned in Sect. 3. We observe that the momentum maps in (a), (b) and (c) are constant up to an error of magnitude 10^{-7}. This number reflects the precision of the iteration algorithm.

Remark 4.2 *The momentum map associated to uniformity is conserved if the grid is chosen in an optimal way. The optimal grid can be determined by an additional set of Euler-Lagrange equations. Since we neglect this aspect here and restrict ourselves to equidistant grids, only seven out of eight possible scalar momentum maps are conserved, confirm Fig. 4 (d).*

For the convergence analysis, a fine discretization with $N = 321$ material points is assumed to be sufficiently precise to serve as a reference solution. We consider convergence of the dis-

crete spacecurve $(r_1 \dots r_N)$ to the reference curve. Here, distances are measured with respect to the norm $\max\{\|r_i\|_2, i = 1 \dots N\}$. In addition, convergence of the director field is analyzed, distances being measured with respect to the norm $\max\{\|R_i\|_F, i = 1 \dots N\}$ using the Frobenius norm $\|\cdot\|_F$. The errorplots obtained from the two-point boundary value problem with $h \in \{\frac{1}{4}, \frac{1}{10}, \frac{1}{40}, \frac{1}{80}\}$ in Fig. 5 show quadratic convergence to the reference configuration. In Ref. [6] we also analyzed convergence to a true analytical solution.

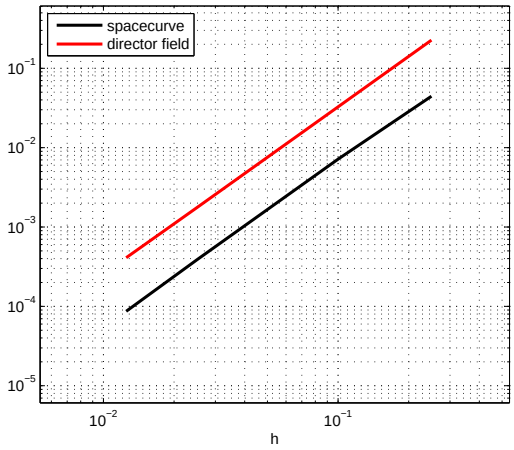

Figure 5: Convergence analysis.

4.2 Two-dimensional equilibria

We consider the two-dimensional example of a hinged frame. An L-shaped extensible and shearable rod is attached at both endpoints such that the tangents are able to move freely (moment free support). This example has previously been discussed in Ref. [12, 13] and all data are taken from there. The length of each leg is $\frac{1}{2}L = 120$ and the stiffness parameters are $GA = 16.62 \cdot 10^6$, $EA = 43.2 \cdot 10^6$, $EI = 14.4 \cdot 10^6$ and $GJ = 11.08 \cdot 10^6$. A vertical force $f = 10^3 \cdot (0, -\lambda)^T$ is applied at position 96 measured from the right upper end.

Motivated by the fact that the interpolation of rotation matrices – appearing e.g. in the discrete strain measures (21) – does not yield proper orthogonal matrices, we modify the discrete rod model by associating the rotation matrices to (the midpoint of) the edges instead of the vertices of the one-dimensional grid. Thus, the discrete configuration comprises only $N-1$ director frames $R_1 \dots R_{N-1}$ which are located *between* the vertices $r_1 \dots r_N$. While the bending and torsional strains (20) remain formally unchanged, the new expression of shear and elongation strains

$$\mathbf{v}_i = \frac{1}{h} R_i^{-1}(r_{i+1} - r_i) \tag{23}$$

involves only one rotation matrix instead of two adjacent rotation matrices' midpoint. As the problem is only two-dimensional, there are two translational degrees of freedom per node and only one rotational degree of freedom specifying the orientation of an edge. We employ the

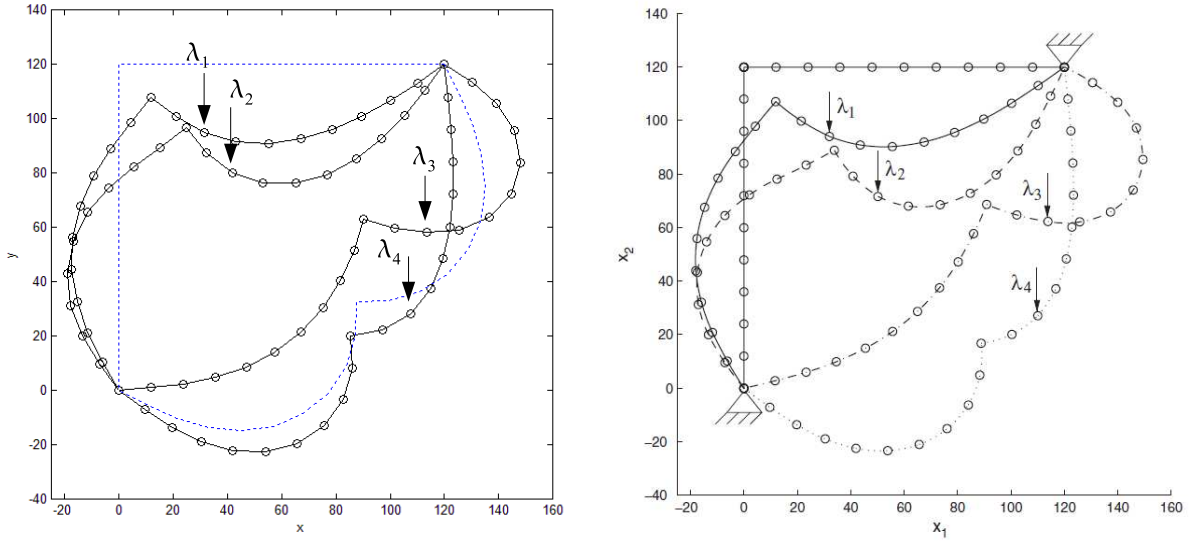

(a) (b)

Figure 6: (a) Deformation of the hinged L-frame corresponding to the load-level parameters $\lambda_1 = 15$, $\lambda_2 = 18.495$, $\lambda_3 = -9.233$ and $\lambda_4 = 21.014$. (b) The results obtained by Betsch and Steinmann (Ref. [12]).

following reparametrization:

$$\begin{pmatrix} x \\ y \end{pmatrix} \mapsto r = \begin{pmatrix} x \\ y \\ 0 \end{pmatrix}$$

$$\alpha \mapsto R = \begin{pmatrix} 0 & \sin(\alpha) & \cos(\alpha) \\ 0 & -\cos(\alpha) & \sin(\alpha) \\ 1 & 0 & 0 \end{pmatrix}$$

and solve for $x_1 \dots x_N, y_1 \dots y_N, \alpha_1 \dots \alpha_{N-1}$. Note however, that the three-dimensional strains (20) and (23) are used to derive the discrete equilibrium equations.

This buckling problem has multiple equilibria, the two stable equilibria are indicated in Fig. 6 (a) by the dashed line. The equlibria can be used to create clever (deformed) initial configurations from which the configurations corresponding to the load-level parameters $\lambda_1 = 15$, $\lambda_2 = 18.495$, $\lambda_3 = -9.233$ and $\lambda_4 = 21.014$, depicted in Fig. 6 (a), can be obtained directly by solving the discrete equilibrium equations iteratively (again Gauss-Newton iteration in the Matlab-funtion `fsolve` has been used). We compare the results from our discrete mechanics model using $N = 21$ vertices to those obtained by Betsch and Steinmann (Ref. [12]) with ten quadratic finite elements and observe small differences in the configurations with high deformation which are probably due to the different factor used in the strains (20) and of course due to the different types of discretization.

To compute the complete load-displacement curve for the node under load (see Fig. 7), a standard arc-length method (described e.g. in [14]) has been employed. Comparing the curve to that obtained in Ref. [12], one can say that the discrete mechanics method captures the qualitative behavior quite well. The differences have to be expected when comparing different methods in an example with relatively coarse discretization.

The resulting material forces and moments are depicted in Fig. 8. Due to the presence of loading, the problem is not frame-indifferent. However, the change in the discrete momentum

maps in Fig. 9 exactly represents the applied loading (up to the numerical tolerance used to solve the equilibrium equations). Note that this is guaranteed by the discrete mechanics approach independent of the number of nodes in the discrete grid.

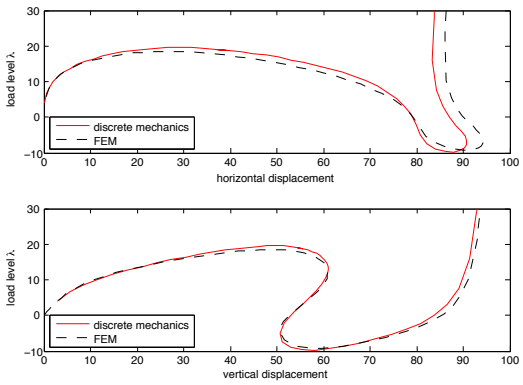

Figure 7: Load-displacement curve of the hinged L-frame.

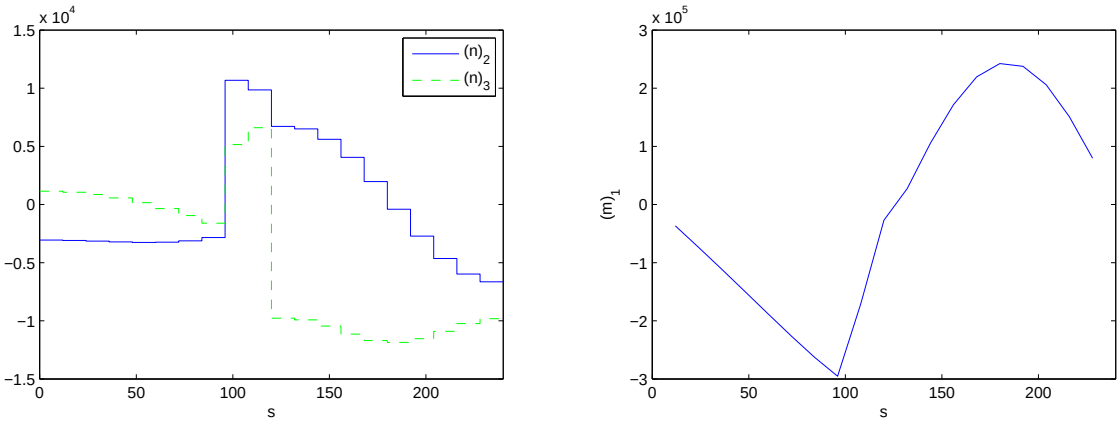

(a) (b)

Figure 8: (a) The discrete forces $\mathbf{n}_i$. (b) The discrete moments $\mathbf{m}_i$.

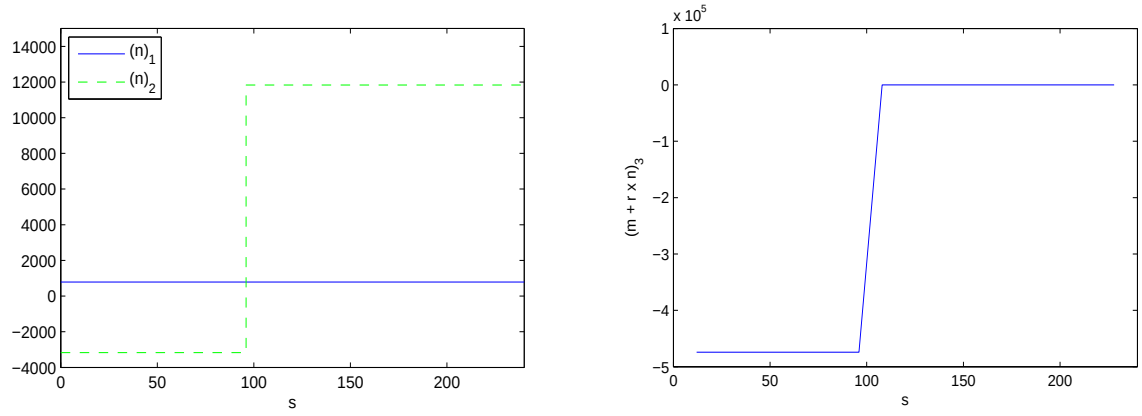

(a) (b)

Figure 9: The discrete momentum maps do change exactly according to the applied load.

5 CONCLUSIONS

This article presents a short introduction to Cosserat rod theory formulated within the (discrete) Lagrangian mechanics context. Both in the continuous and in the discrete setting, we started from a variational principle from which the theory and solution methods were developed.

By treating a rod as a Lagrangian system on $\mathbb{R}^3 \times \mathrm{SO}(3)$ we obtained the equilibrium equations as Euler-Lagrange equations corresponding to the potential energy functional. Noether's theorem provides a constructive tool and a complete mathematical theory to identify and compute first integrals. This is especially useful in the discrete setting, where the expressions for the discrete moments can be quite complicated. Moreover, we were able to show that the discrete Euler-Lagrange equations always yield the "natural" discretization in Eq. (13) of the spatial equilibrium equations – derivatives being replaced by differences – which is due to frame-indifference of the discrete internal energy. Various boundary conditions can be implemented very easily (some other numerical tools are doing quite hard on boundary value problems).

Our numerical experiments showed that discrete momentum maps are conserved with high accuracy, which is the benefit of the discrete mechanics appoach. The theory from Sect. 3 can be extended to non-uniform rods and then, by construction, deals with non-equidistant grids. However, this leads to an extended set of discrete Euler-Lagrange equations and it becomes much harder to find solution strategies. This aspect is subject to current research. In addition, a more detailed comparison with the finite element approach would be interesting.

6 ACKNOWLEDGEMENTS

We would like to thank P. Betsch for providing the data used for comparison in Sect. 4.2.

REFERENCES

[1] J. E. Marsden, M. West. Discrete mechanics and variational integrators. *Acta Numerica*, 357–514, 2001.

[2] S. Kehrbaum, J. H. Maddocks. Elastic rods, rigid bodies, quaternions and the last quadrature. *Philosophical Transactions of the Royal Society of London, Series A*, **355**(1732), 2117–2136, 1997.

[3] N. Chouaieb, J. H. Maddocks. Kirchhoff's problem of helical equilibria of uniform rods, *Journal of Elasticity*, **77**, 221–247, 2004.

[4] A. I. Bobenko, Y. B. Suris. Discrete time Lagrangian mechanics on Lie groups, with an application on the Lagrange top. *Communications in Mathematical Physics* 1999, **204**, 147–188, 1999.

[5] M. F. Dixon. *Geometric integrators for continuum dynamics*. PhD thesis, Imperial College, London, 2007.

[6] P. Jung. *A discrete mechanics approach to Cosserat rod theory – Static equilibria*. Diploma thesis, University of Kaiserslautern, 2009.

[7] P. Betsch. The discrete null space method for the energy consistent integration of constrained mechanical systems. Part I: Holonomic constraints. *Computer Methods in Applied Mechanics and Engineering*, **194**, 5159–5190, 2005.

[8] S. Leyendecker, P. Betsch, P. Steinmann. The discrete null space method for the energy consistent integration of constrained mechanical systems. Part III: Flexible multibody dynamics. *Multibody System Dynamics*, **19**, 45–72, 2008.

[9] S. Leyendecker, J. E. Marsden, M. Ortiz. Variational integrators for constrained dynamical systems. *Zeitschrift für Angewandte Mathematik und Mechanik*, **88**(9), 677–708, 2008.

[10] J. C. Simo. A finite strain beam formulation. The three-dimensional dynamic problem - Part I. *Computer Methods in Applied Mechanics and Engineering*, **49**, 55–70, 1985.

[11] S. S. Antman. *Nonlinear Problems of Elasticity* (2nd edn). Springer, 2005.

[12] P. Betsch, P. Steinmann. Frame-indifferent beam finite elements based upon the geometrically exact beam theory. *International Journal of Numerical Methods in Engineering*, **54**, 1775–1788, 2002.

[13] J. C. Simo, L. Vu-Quoc. A three-dimensional finite-strain rod model - Part II Computational aspects. *Computer Methods in Applied Mechanics and Engineering*, **58**, 79–116, 1986.

[14] M.A. Crisfield. *Non-linear Finite Element Analysis of Solids and Structures. Volume I: Essentials*. Wiley, 1991.